Rapid Communications

Impact of exciton delocalization on exciton-vibration interactions in organic semiconductors

Antonios M. Alvertis,[1,*] Raj Pandya,[1] Loreta A. Muscarella,[2] Nipun Sawhney,[1] Malgorzata Nguyen,[1] Bruno Ehrler,[2] Akshay Rao,[1] Richard H. Friend,[1] Alex W. Chin,[3] and Bartomeu Monserrat[1,4,†]

[1]*Cavendish Laboratory, University of Cambridge, J. J. Thomson Avenue, Cambridge CB3 0HE, United Kingdom*
[2]*AMOLF, Center for Nanophotonics, Science Park 104, 1098 XG Amsterdam, The Netherlands*
[3]*CNRS and Institut des NanoSciences de Paris, Sorbonne Université, 75252 Paris Cedex 05, France*
[4]*Department of Materials Science and Metallurgy, University of Cambridge, 27 Charles Babbage Road, Cambridge CB3 0FS, United Kingdom*

(Received 25 May 2020; accepted 12 August 2020; published 31 August 2020)

Organic semiconductors exhibit properties of individual molecules and extended crystals simultaneously. The strongly bound excitons they host are typically described in the molecular limit, but excitons can delocalize over many molecules, raising the question of how important the extended crystalline nature is. Using accurate Green's function based methods for the electronic structure and nonperturbative finite difference methods for exciton-vibration coupling, we describe exciton interactions with molecular and crystal degrees of freedom concurrently. We find that exciton delocalization controls these interactions, with thermally activated crystal phonons predominantly coupling to delocalized states, and molecular quantum fluctuations predominantly coupling to localized states. Based on this picture, we quantitatively predict and interpret the temperature and pressure dependence of excitonic peaks in the acene series of organic semiconductors, which we confirm experimentally, and we develop a simple experimental protocol for probing exciton delocalization. Overall, we provide a unified picture of exciton delocalization and vibrational effects in organic semiconductors, reconciling the complementary views of finite molecular clusters and periodic molecular solids.

DOI: 10.1103/PhysRevB.102.081122

Optoelectronic devices based on organic semiconductors (OSCs), such as light-emitting diodes (LEDs) [1] and solar cells [2], are promising candidates for technological applications. In contrast to their inorganic counterparts, OSCs host strongly bound excitons [3,4] that, depending on the relative spin of the electron and hole pair, form spin-zero (singlet) or spin-one (triplet) configurations. The interconversion between singlet and triplet states is of high relevance to the application of OSCs, with examples including thermally activated delayed fluorescence used in organic LEDs [5,6], and singlet exciton fission which could lead to solar cells with efficiencies surpassing the Shockley-Queisser limit [7–9].

The weak van der Waals interaction between molecules in OSCs has led to the common approximation of using isolated molecular dimers or oligomers to simulate the entire crystal [10–13]. Wave-function-based methods are the natural way of studying such finite-sized clusters of molecules, providing a good description of the underlying physics in those systems where exciton states are localized. While triplet excitons are localized in most cases, the exchange interaction drives singlet excitons to delocalize over multiple monomers [14,15]. Therefore, OSCs can simultaneously exhibit features of the molecular and extended crystal limits, calling for a unified picture.

Due to the mechanically soft character of organic materials, the coupling of excitons to molecular and crystal vibrations can be extremely strong and dominate the physics that makes OSCs interesting from an application point of view. For example, exciton-vibration coupling has been shown to play a central role in processes such as singlet fission and exciton transport [16–18], and several theoretical studies have successfully captured this interaction in molecular clusters [19–21]. However, these molecule-based approaches cannot capture the long-range intermolecular vibrations that lead to strong deviations of the orbital overlap between neighboring monomers [22,23]. A full treatment of exciton delocalization becomes necessary to account for the strong dynamic disorder of OSCs in solid-state systems, but this remains an open challenge.

In this work, we present a theoretical framework to understand exciton-phonon interactions in OSCs treating molecular and crystal features on the same footing. We combine many-body *GW* and Bethe-Salpeter calculations for exciton properties [24–26] with finite displacement methods for vibrational properties [27,28] to capture the strong nonperturbative exciton-vibration interactions present in OSCs [29]. This combination of highly accurate methods allows us to identify the extent of exciton localization as the key parameter determining the relative importance of molecular and crystal degrees of freedom, providing a unified picture between the molecular and crystal limits of OSCs. Our framework has multiple implications for the properties of these materials, some examples of which we explore. We uncover the

*ama80@cam.ac.uk
†bm418@cam.ac.uk

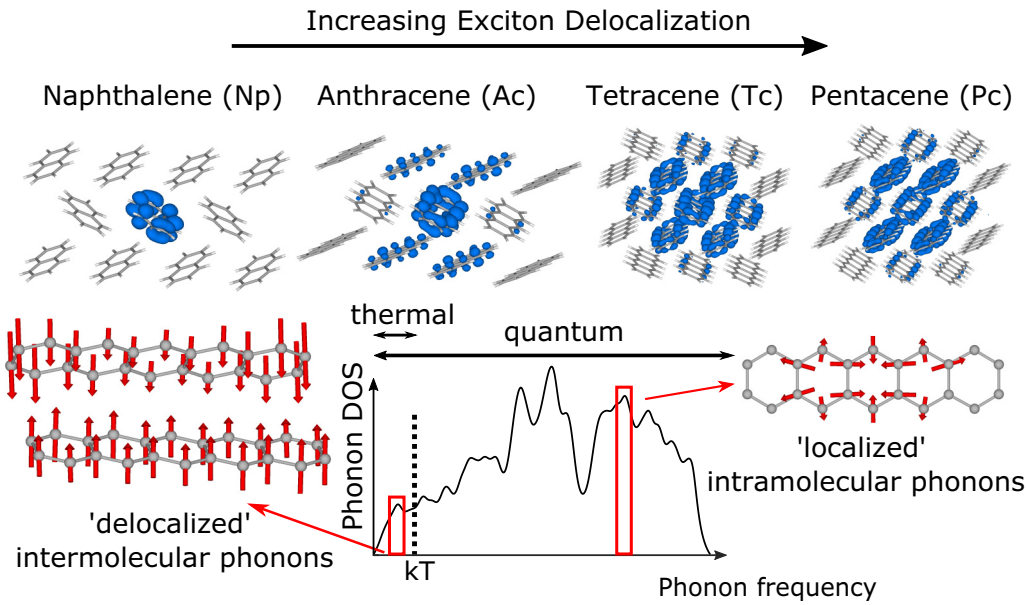

FIG. 1. Singlet excitons in the acene series of molecular crystals range from entirely localized (naphthalene) to highly delocalized (pentacene). The phonon density of states (DOS) of these materials consists of a thermally activated regime of intermolecular motions, and a high-energy regime of intramolecular modes that are only active due to quantum fluctuations. The interaction of delocalized excitons is dominated by low-energy thermally active modes, while localized excitons couple preferentially to high-energy modes via quantum fluctuations.

microscopic mechanism for the weak temperature dependence of excitons in the acene series of OSCs, rigorously comparing against our experimental measurements. We also find that nuclear quantum fluctuations lead to strong exciton energy renormalization, and accounting for this effect allows for unprecedented predictive power for *absolute* exciton energies compared to experiment. Finally, we predict that delocalized excitons should exhibit stronger pressure dependencies than localized ones, and again quantitatively confirm this prediction with experiments in the acene series.

At temperature T, we include the phonon contribution to the exciton energy $E_{\mathrm{exc}}(T)$ by means of the quantum-mechanical expectation value:

$$E_{\mathrm{exc}}(T) = \frac{1}{\mathcal{Z}} \sum_{\mathbf{s}} \langle \chi_{\mathbf{s}}(\mathbf{u}) | E_{\mathrm{exc}}(\mathbf{u}) | \chi_{\mathbf{s}}(\mathbf{u}) \rangle e^{-E_{\mathbf{s}}/k_{\mathrm{B}}T}, \qquad (1)$$

where $|\chi_{\mathbf{s}}\rangle$ is the harmonic vibrational wave function in state $\mathbf{s}$ with energy $E_{\mathbf{s}}$, $\mathcal{Z} = \sum_{\mathbf{s}} e^{-E_{\mathbf{s}}/k_{\mathrm{B}}T}$ is the partition function, and $\mathbf{u}$ is a collective coordinate that includes the amplitudes of all normal modes of vibration in the system. We evaluate Eq. (1) by generating stochastic samples distributed according to the harmonic vibrational ensemble, calculating the exciton energy and averaging over all configurations. More details on the computational methodology are provided in the Supplemental Material (SM) [30]. Here we emphasize that while individual phonon modes are treated within the harmonic approximation, our methodology still captures exciton-phonon interactions to all orders as it does not rely on a perturbative treatment of the coupling.

To probe our theoretical framework, we use the acene series of molecular crystals because they exhibit singlet excitons that range from entirely localized (molecular limit) to strongly delocalized (crystal limit), as visualized in Fig. 1. The electron density is shown in blue for a hole localized on the central monomer of the displayed area. Throughout the rest of this Rapid Communication, the term delocalization will refer to the spatial extent of the electron wave function for a hole localized at a specific point. For singlet excitonic states, molecular size determines the degree of delocalization in the solid state [14]. For large organic structures, the average electron-hole distance on a single molecule is comparable to the distance between neighboring molecules. Therefore, the attractive Coulomb energy between electron and hole is similar when they localize on the same or on adjacent molecules, allowing for delocalized states with large average electron-hole separation. In contrast, in small molecules the attractive Coulomb interaction of electron and hole within a single molecule is significantly stronger than if they localized on different molecules, leading to localized singlet excitons. Triplet excitons are generally more localized than singlets, due to the lack of a repulsive exchange interaction in this state [26]. The triplet wave functions of the acene crystals are visualized in SM Fig. S1 [30]. Therefore, depending on spin and on the size of molecules, different degrees of exciton delocalization appear in the solid state.

By employing Eq. (1), we obtain the expectation value for the singlet and triplet exciton energies of the acene crystals at 0 and 300 K arising from exciton-phonon coupling. The interaction of the exciton with phonons leads to a redshift of its energy, due to the stabilizing character of intraband phonon-induced transitions [31]. Even at 0 K, phonon quantum fluctuations with an energy of $\frac{1}{2}\hbar\omega$ interact with the exciton, leading to a redshift of its energy compared to a static picture. This effect becomes more pronounced for the smaller acenes (fewer number of carbon rings), where excitons are

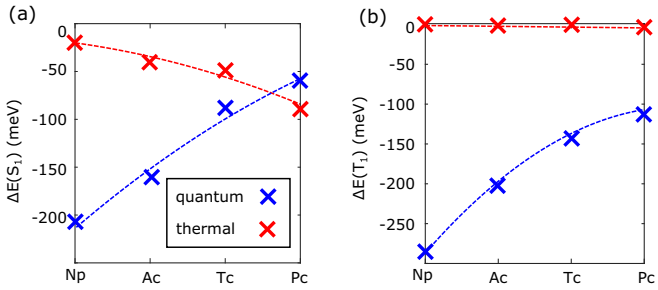

FIG. 2. Change caused by thermal activation (red) and quantum fluctuations (blue) of phonons to the singlet [panel (a)] and triplet [panel (b)] exciton energies of the different acenes.

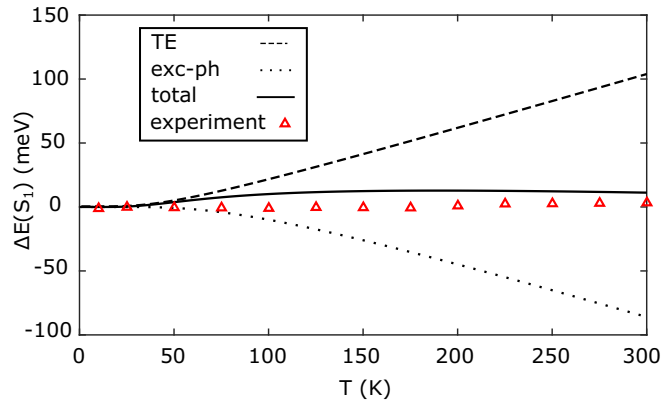

FIG. 3. Experimental (red triangles) and theoretical (black solid line) temperature-dependent absorption of pentacene. The dashed and dotted lines indicate the individual effects of thermal expansion (TE) and exciton-phonon coupling on the singlet energy.

more localized, as visualized in Fig. 2. Comparing the singlet [panel (a)] to the triplet [panel (b)], the redshift is more important for the more localized triplet states. By increasing the temperature from 0 to 300 K, low-energy intermolecular motions are activated, leading to a further redshift of exciton energies. We find this effect to be more important for more delocalized states. Indeed thermally activated phonons have a negligible effect on the energy of the highly localized triplet states. Overall, in the molecular limit, excitons couple preferentially to high-energy phonons that are not thermally activated, so the coupling is purely via quantum fluctuations. By contrast, in the crystal limit thermally activated low-energy phonons dominate the interaction with excitons. In intermediate cases, both contributions can be important.

To understand these results, let us consider the form of the phonon density of states (DOS) in OSCs, schematically presented in Fig. 1. This consists of two distinct regions: a small thermally activated regime of low-frequency phonons, corresponding to intermolecular motion, and a large region which is dominated by high-energy intramolecular motions, such as C-C stretches. While most of the phonon modes that fall into the latter regime are not thermally activated, they still oscillate with their zero-point energy. Thermally activated modes that modulate the orbital overlap between neighboring monomers [22,23] will predominantly have an effect on more delocalized excitons, the properties of which depend on intermolecular interactions, due to their wave function extending over a larger number of molecules. Similarly, one expects that the high-energy intramolecular motions that are only active due to quantum fluctuations, will mostly affect localized excitons, the wave function of which has a greater amplitude in the vicinity of these localized motions. Therefore, based on the extent of their delocalization, excitons in OSCs respond differently to the different kinds of vibrations present in these materials. We now proceed to apply this intuitive picture summarized in Fig. 1 to uncover the mechanism behind the temperature-dependent properties of excitons.

The redshift of the exciton energy relative to its value at 0 K and due to thermally activated phonons is visualized in Fig. 3 for the case of pentacene (dotted line). However, exciton-phonon coupling is not enough to capture the experimentally observed temperature dependence of the exciton energy (red triangles in Fig. 3), and must be complemented by the effect of thermal expansion (TE, dashed line). Thermal expansion increases intermolecular distances, thus approaching the limit of isolated single molecules, and hence entirely localized excitons. This destabilizes the exciton energy, an effect which is more pronounced for delocalized singlets, and less important for states that are relatively localized to begin with. In principle, it is possible to obtain the effects of thermal expansion from first principles using the quasiharmonic approximation [32], within which the free energy of the system calculated at the harmonic level is minimized as a function of volume. However, this is computationally expensive for systems like the acene crystals with several independent lattice parameters. Instead, we perform exciton calculations on a range of experimental structures obtained at different temperatures, as outlined in section S4 of the SM [30].

The effects of thermal expansion and exciton-phonon coupling almost perfectly cancel out, leading to largely temperature-independent exciton energies (solid line), in excellent agreement with experiment. While exciton delocalization determines the magnitude of these two effects individually, the net temperature dependence of the exciton energies is overall weak, something which is also true for tetracene, anthracene, and naphthalene, the results for which are given in the SM [30]. As discussed in detail in Sec. S10 of the SM [30], the small differences between the computational and experimental results are mainly due to the challenge associated with accounting for the effects of very long-wavelength phonons on excitons, as well as the deviation of some of these modes from the harmonic behavior that our methodology assumes.

The blueshift of exciton energies due to thermal expansion is caused by the increase in intermolecular distances, while the redshift that results from exciton-phonon coupling is due to the dominance of intraband over interband phonon-induced transitions [31]. Both these effects hold in most molecular crystals, unless one considers special cases with anomalous thermal expansion or very small optical gaps, respectively. Therefore, we expect the cancellation of the effects of thermal expansion and exciton-phonon coupling to be present in the vast majority of OSCs, leading to overall weak temperature dependence of exciton energies.

Since the effect of thermal fluctuations on exciton energies is small, it is quantum fluctuations that are mostly responsible

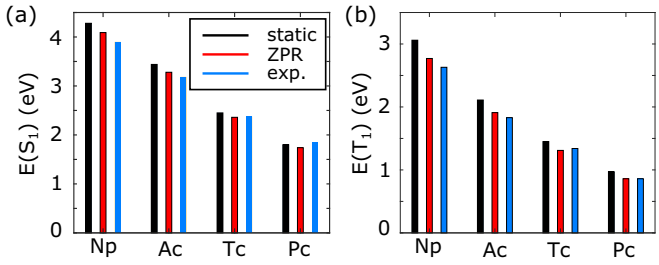

FIG. 4. Comparison of the computed static exciton energies obtained to their zero-point renormalized (ZPR) values and to experiment. See SM Sec. S3 [30] for the tabulated data.

for redshifting their values from those of a static lattice. This leads to a greatly improved agreement between theory and experiment as summarized in Fig. 4 and Table S1, highlighting the predictive power of our approach. This result is particularly important for triplet states, the energy of which is experimentally very challenging to determine [6,33]; the correction to the static values for these states is significant due to their highly localized character and associated coupling to the high-frequency modes that are active due to quantum fluctuations. This strong renormalization of exciton energies due to quantum fluctuations is an inherent characteristic of OSCs due to the light weight of their constituent elements, and thus the high frequency of oscillations they exhibit. Therefore, accounting for this effect is crucial, regardless of the accuracy of the underlying electronic structure method. The accurate calculation of exciton energies is crucial to various photophysical processes in OSCs. For the example of singlet fission, we successfully predict the experimentally well-established exothermicity $[E(S_1) > 2E(T_1)]$ of singlet fission in solid pentacene [34], which is not captured by many-body perturbation theory in the absence of quantum fluctuations [15,35]. We also capture the endothermicity of singlet fission in tetracene [36].

The magnitude of the effect of thermal expansion and exciton-phonon coupling on exciton energies depends on the degree of wave-function delocalization. Unfortunately, the cancellation of these effects that we have demonstrated does not allow one to utilize them as a means of probing delocalization experimentally. Nevertheless, the insights from the above discussion motivate us to examine the effect of pressure on exciton energies. The application of hydrostatic pressure at a given temperature reduces the volume V_o of the unit cell at atmospheric pressure ($\Delta V/V_o < 0$), an effect *opposite* to thermal expansion, which increases the unit cell volume ($\Delta V/V_o > 0$). However, unlike thermal expansion, the effect of pressure does not compete with phonon-activated processes, leading to a strong redshift of exciton energies [37], an effect that we expect to be stronger for more delocalized states, and could hence be used to probe delocalization. For obtaining the exciton properties at finite pressures, we relax both the internal structure and volume of the unit cell, minimizing the enthalpy at a given pressure. For each acene crystal, and as outlined in detail in Secs. S3 and S4 of the SM [30], we compute the exciton properties at 0, 0.5, 1, 2, 4, and 5 GPa, also accounting for the change in the effect of phonon quantum fluctuations under pressure.

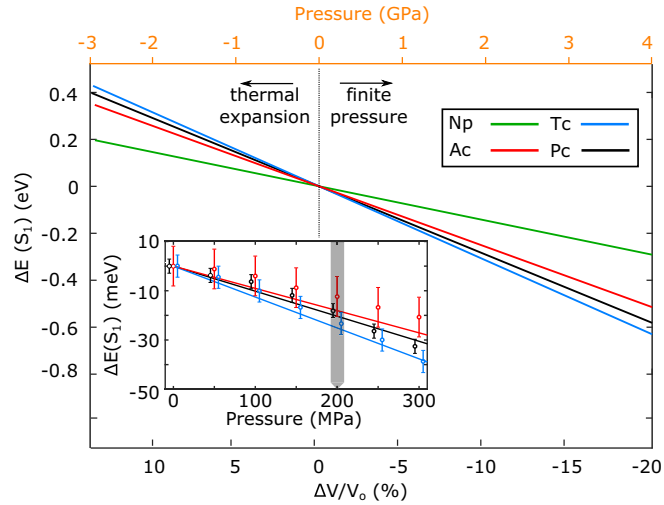

FIG. 5. Theoretical volume and pressure dependence of exciton energies. We compare to pressure-dependent measurements within 0–300 MPa in the inset.

Figure 5 shows the change of the singlet energy of the acene crystals as a function of unit cell volume. As argued previously, changes in intermolecular distances induced by pressure or thermal expansion have a stronger effect on delocalized states. Indeed, we find that for naphthalene the singlet volume dependence is weaker than for anthracene, which in turn is weaker than that of tetracene. Interestingly, pentacene has a slightly weaker volume dependence than tetracene, which is due to qualitative changes in the effect of phonon quantum fluctuations at finite pressures. Consistent with this picture, we find in Fig. S2 that the pressure dependence of the triplet energies is significantly weaker, due to the highly localized nature of these states. In the inset of Fig. 5, we compare our theoretical predictions for the change of the singlet energies at finite pressure to experiment, in the range of 0–300 MPa. The full experimental spectra are given in Fig. S8. We find that theory and experiment are in very good agreement and, remarkably, we correctly predicted the unconventional pressure dependence for pentacene, confirming the accuracy of our theoretical framework.

The above discussion shows that the slope of the experimental exciton energy pressure dependence provides a qualitative measure of exciton delocalization. Additionally, in combination with the experimentally measured exciton temperature dependence, it can also be used to provide an estimate of the magnitude of exciton-phonon interactions due to thermal fluctuations. The shift of exciton energies upon compression $\Delta V/V_o < 0$ is linear, and can be extrapolated to $\Delta V/V_o > 0$, hence providing an expected blueshift of the exciton energy due to thermal expansion. The difference of this expected blueshift from the experimentally measured energy shift (compared to 0 K) gives the magnitude of exciton energy renormalization due to coupling to thermally activated low-frequency phonons. This is complementary to extracting the magnitude of exciton-phonon interactions from the vibronic progression of the absorption spectrum [38], as the latter only provides information on the coupling of the exciton to high-frequency modes.

We propose a general framework to study exciton-phonon interactions in organic semiconductors describing localized molecular and extended crystal degrees of freedom simultaneously. We show that exciton delocalization determines the magnitude and nature of these interactions: localized excitons predominantly couple to high-frequency modes via quantum fluctuations, while delocalized excitons interact more strongly with thermally activated low-frequency phonons. Together with the effect of thermal expansion, which also depends on exciton delocalization, this allows us to reveal the full microscopic mechanism behind the weak temperature of exciton energies in acene crystals, and argue that this should hold in the vast majority of molecular crystals. As a consequence of the weak temperature dependence, the major contribution to exciton energy renormalization compared to the static lattice arises from quantum fluctuations of mostly high-frequency vibrations, always present in organic materials. The magnitude of this renormalization also depends sensitively on exciton delocalization, and accounting for this effect is necessary in order to achieve predictive power for exciton energies.

Overall, our framework provides a unifying picture between the molecular and crystal limits of organic semiconductors, showing how the delocalization of excitons determines their response to a wide range of structural changes, beyond lattice vibrations and thermal expansion. The effect of pressure provides such an example, and we find that pressure-dependent measurements may be used as a probe of delocalization and thermally activated exciton-phonon interactions. Therefore, based on factors that determine exciton delocalization, such as spin and the size of molecules, one can anticipate the difference in the response of different materials to a variety of structural changes.

The data underlying this publication can be found in [56].

A.M.A. thanks Jeffrey B. Neaton, Jonah B. Haber, Felipe H. da Jornada, and Christoph Schnedermann for insightful discussions. The authors acknowledge the support of the Winton Programme for the Physics of Sustainability. A.M.A. acknowledges the support of the Engineering and Physical Sciences Research Council for funding under Grant No. EP/L015552/1. The work of L.A.M. and B.E. is part of the Dutch Research Council (NWO) and was performed at the research institute AMOLF, supported by NWO Vidi Grant No. 016.Vidi.179.005. R.H.F. acknowledges the Simons Foundation Grant No. 601946. A.W.C. acknowledges financial support from Agence Nationale de la Recherche (Grant No. ANR-19-CE24-0028). B.M. acknowledges support from the Gianna Angelopoulos Programme for Science, Technology, and Innovation. Part of the calculations were performed using resources provided by the Cambridge Tier-2 system operated by the University of Cambridge Research Computing Service [57] and funded by EPSRC Tier-2 capital Grant No. EP/P020259/1.

[1] S. Reineke, F. Lindner, G. Schwartz, N. Seidler, K. Walzer, B. Lüssem, and K. Leo, White organic light-emitting diodes with fluorescent tube efficiency, Nature (London) **459**, 234 (2009).

[2] L. Meng, Y. Zhang, X. Wan, C. Li, X. Zhang, Y. Wang, X. Ke, Z. Xiao, L. Ding, R. Xia, H.-L. Yip, Y. Cao, and Y. Chen, Organic and solution-processed tandem solar cells with 17.3% efficiency, Science **361**, 1094 (2018).

[3] M. Knupfer, Exciton binding energies in organic semiconductors, Appl. Phys. A **77**, 623 (2003).

[4] A. Köhler and H. Bässler, Triplet states in organic semiconductors, Mater. Sci. Eng., R **66**, 71 (2009).

[5] H. Uoyama, K. Goushi, K. Shizu, H. Nomura, and C. Adachi, Highly efficient organic light-emitting diodes from delayed fluorescence, Nature (London) **492**, 234 (2012).

[6] S. Reineke and M. A. Baldo, Room temperature triplet state spectroscopy of organic semiconductors, Sci. Rep. **4**, 3797 (2014).

[7] M. B. Smith and J. Michl, Singlet fission, Chem. Rev. **110**, 6891 (2010).

[8] M. C. Hanna and A. J. Nozik, Solar conversion efficiency of photovoltaic and photoelectrolysis cells with carrier multiplication absorbers, J. Appl. Phys. **100**, 074510 (2006).

[9] A. Rao and R. H. Friend, Harnessing singlet exciton fission to break the Shockley-Queisser limit, Nat. Rev. Mater. **2**, 17063 (2017).

[10] D. Beljonne, H. Yamagata, J. L. Brédas, F. C. Spano, and Y. Olivier, Charge-Transfer Excitations Steer the Davydov Splitting and Mediate Singlet Exciton Fission in Pentacene, Phys. Rev. Lett. **110**, 226402 (2013).

[11] T. C. Berkelbach, M. S. Hybertsen, and D. R. Reichman, Microscopic theory of singlet exciton fission. II. Application to pentacene dimers and the role of superexchange, J. Chem. Phys. **138**, 114103 (2013).

[12] S. R. Yost, J. Lee, M. W. B. Wilson, T. Wu, D. P. McMahon, R. R. Parkhurst, N. J. Thompson, D. N. Congreve, A. Rao, K. Johnson, M. Y. Sfeir, M. G. Bawendi, T. M. Swager, R. H. Friend, M. A. Baldo, and T. Van Voorhis, A transferable model for singlet-fission kinetics, Nat. Chem. **6**, 492 (2014).

[13] P. B. Coto, S. Sharifzadeh, J. B. Neaton, and M. Thoss, Low-lying electronic excited states of pentacene oligomers: A comparative electronic structure study in the context of singlet fission, J. Chem. Theory Comput. **11**, 147 (2015).

[14] P. Cudazzo, F. Sottile, A. Rubio, and M. Gatti, Exciton dispersion in molecular solids, J. Phys.: Condens. Matter **27**, 113204 (2015).

[15] S. Refaely-Abramson, F. H. da Jornada, S. G. Louie, and J. B. Neaton, Origins of Singlet Fission in Solid Pentacene from an *ab initio* Green's Function Approach, Phys. Rev. Lett. **119**, 267401 (2017).

[16] J. Aragó and A. Troisi, Dynamics of the Excitonic Coupling in Organic Crystals, Phys. Rev. Lett. **114**, 026402 (2015).

[17] A. J. Musser, M. Liebel, C. Schnedermann, T. Wende, T. B. Kehoe, A. Rao, and P. Kukura, Evidence for conical intersection dynamics mediating ultrafast singlet exciton fission, Nat. Phys. **11**, 352 (2015).

[18] A. A. Bakulin, S. E. Morgan, T. B. Kehoe, M. W. Wilson, A. W. Chin, D. Zigmantas, D. Egorova, and A. Rao, Real-time observation of multiexcitonic states in ultrafast singlet fission

using coherent 2D electronic spectroscopy, Nat. Chem. **8**, 16 (2016).

[19] K. Miyata, Y. Kurashige, K. Watanabe, T. Sugimoto, S. Takahashi, S. Tanaka, J. Takeya, T. Yanai, and Y. Matsumoto, Coherent singlet fission activated by symmetry breaking, Nat. Chem. **9**, 983 (2017).

[20] C. Schnedermann, A. M. Alvertis, T. Wende, S. Lukman, J. Feng, F. A. Y. N. Schröder, D. H. P. Turban, J. Wu, N. D. M. Hine, N. C. Greenham, A. W. Chin, A. Rao, P. Kukura, and A. J. Musser, A molecular movie of ultrafast singlet fission, Nat. Commun. **10**, 4207 (2019).

[21] A. M. Alvertis, F. A. Schröder, and A. W. Chin, Non-equilibrium relaxation of hot states in organic semiconductors: Impact of mode-selective excitation on charge transfer, J. Chem. Phys. **151**, 084104 (2019).

[22] A. Troisi, G. Orlandi, and J. E. Anthony, Electronic interactions and thermal disorder in molecular crystals containing cofacial pentacene units, Chem. Mater. **17**, 5024 (2005).

[23] A. Troisi and G. Orlandi, Dynamics of the intermolecular transfer integral in crystalline organic semiconductors, J. Phys. Chem. A **110**, 4065 (2006).

[24] H. Lars, New method for calculating the one-particle green's function with application to the electron-gas problem, Phys. Rev. **139**, A796 (1965).

[25] M. Rohlfing and S. G. Louie, Electron-Hole Excitations in Semiconductors and Insulators, Phys. Rev. Lett. **81**, 2312 (1998).

[26] M. Rohlfing and S. G. Louie, Electron-hole excitations and optical spectra from first principles, Phys. Rev. B **62**, 4927 (2000).

[27] K. Kunc and R. M. Martin, *Ab Initio* Force Constants of GaAs: A New Approach to Calculation of Phonons and Dielectric Properties, Phys. Rev. Lett. **48**, 406 (1982).

[28] B. Monserrat, Electron-phonon coupling from finite differences, J. Phys.: Condens. Matter **30**, 083001 (2018).

[29] B. Monserrat, Vibrational averages along thermal lines, Phys. Rev. B **93**, 014302 (2016).

[30] See Supplemental Material at http://link.aps.org/supplemental/10.1103/PhysRevB.102.081122 for additional figures and details on the computational and experimental methodology, which includes Refs. [6,27,34,37,39–55].

[31] K. Saha and I. Garate, Phonon-induced topological insulation, Phys. Rev. B **89**, 205103 (2014).

[32] N. Mounet and N. Marzari, First-principles determination of the structural, vibrational and thermodynamic properties of diamond, graphite, and derivatives, Phys. Rev. B **71**, 205214 (2005).

[33] B. Ehrler, B. J. Walker, M. L. Böhm, M. W. Wilson, Y. Vaynzof, R. H. Friend, and N. C. Greenham, *In situ* measurement of exciton energy in hybrid singlet-fission solar cells, Nat. Commun. **3**, 1019 (2012).

[34] A. Rao, M. W. B. Wilson, S. Albert-Seifried, R. Di Pietro, and R. H. Friend, Photophysics of pentacene thin films: The role of exciton fission and heating effects, Phys. Rev. B **84**, 195411 (2011).

[35] X. Liu, R. Tom, X. Wang, C. Cook, B. Schnatschneider, and N. Marom, Pyrene-stabilized acenes as intermolecular singlet fission candidates: Importance of exciton wave-function convergence, J. Phys.: Condens. Matter **32**, 184001 (2020).

[36] J. J. Burdett and C. J. Bardeen, The dynamics of singlet fission in crystalline tetracene and covalent analogs, Acc. Chem. Res. **46**, 1312 (2013).

[37] L. Farina, K. Syassen, A. Brillante, R. G. Della Valle, E. Venuti, and N. Karl, Pentacene at high pressure, High Press. Res. **23**, 349 (2003).

[38] F. C. Spano, The spectral signatures of Frenkel polarons in H- and J-aggregates, Acc. Chem. Res. **43**, 429 (2010).

[39] P. Giannozzi, S. Baroni, N. Bonini, M. Calandra, R. Car, C. Cavazzoni, D. Ceresoli, G. L. Chiarotti, M. Cococcioni, I. Dabo *et al.*, QUANTUM ESPRESSO: A modular and open-source software project for quantum simulations of materials, J. Phys.: Condens. Matter **21**, 395502 (2009).

[40] S. Haas, B. Batlogg, C. Besnard, M. Schiltz, C. Kloc, and T. Siegrist, Large uniaxial negative thermal expansion in pentacene due to steric hindrance, Phys. Rev. B **76**, 205203 (2007).

[41] J. M. Robertson, V. C. Sinclair, and J. Trotter, The crystal and molecular structure of tetracene, Acta Crystallogr. **14**, 697 (1961).

[42] J. G. Malecki, CCDC 950158 (2014), doi: 10.5517/cc10wq8w.

[43] S. C. Capelli, A. Albinati, S. A. Mason, and B. T. Willis, Molecular motion in crystalline naphthalene: Analysis of multi-temperature X-ray and neutron diffraction data, J. Phys. Chem. A **110**, 11695 (2006).

[44] A. Tkatchenko and M. Scheffler, Accurate Molecular Van der Waals Interactions from Ground-State Electron Density and Free-Atom Reference Data, Phys. Rev. Lett. **102**, 073005 (2009).

[45] D. Sangalli, A. Ferretti, H. Miranda, C. Attaccalite, I. Marri, E. Cannuccia, P. Melo, M. Marsili, F. Paleari, A. Marrazzo *et al.*, Many-body perturbation theory calculations using the yambo code, J. Phys.: Condens. Matter **31**, 325902 (2019).

[46] O. Schnepp, Electronic spectra of molecular crystals, Annu. Rev. Phys. Chem. **14**, 35 (1963).

[47] M. W. Wilson, A. Rao, K. Johnson, S. Gélinas, R. Di Pietro, J. Clark, and R. H. Friend, Temperature-independent singlet exciton fission in tetracene, J. Am. Chem. Soc. **135**, 16680 (2013).

[48] P. Swiderek, M. Michaud, G. Hohlneicher, and L. Sanche, Electron energy loss spectroscopy of solid naphthalene and acenaphthene: Search for the low-lying triplet states, Chem. Phys. Lett. **175**, 667 (1990).

[49] A. Rao, M. W. Wilson, J. M. Hodgkiss, S. Albert-Seifried, H. Bässler, and R. H. Friend, Exciton fission and charge generation via triplet excitons in pentacene/C_{60} bilayers, J. Am. Chem. Soc. **132**, 12698 (2010).

[50] C. P. Brock and J. D. Dunitz, Temperature dependence of thermal motion in crystalline anthracene, Acta Crystallogr. Sect. B: Struct. Sci., Cryst. Eng. Mater. **46**, 795 (1990).

[51] D. Holmes, S. Kumaraswamy, A. J. Matzger, and K. P. C. Vollhardt, On the nature of nonplanarity in the [N]phenylenes, Chem. Eur. J. **5**, 3399 (1999).

[52] R. B. Campbell, J. M. Robertson, and J. Trotter, The crystal structure of hexacene, and a revision of the

crystallographic data for tetracene, Acta Crystallogr. **15**, 289 (1962).

[53] J. H. Lloyd-Williams and B. Monserrat, Lattice dynamics and electron-phonon coupling calculations using nondiagonal supercells, Phys. Rev. B **92**, 184301 (2015).

[54] K. Momma and F. Izumi, VESTA 3 for three-dimensional visualization of crystal, volumetric and morphology data, J. Appl. Crystallogr. **44**, 1272 (2011).

[55] B. Monserrat, Correlation effects on electron-phonon coupling in semiconductors: Many-body theory along thermal lines, Phys. Rev. B **93**, 100301(R) (2016).

[56] A. Alvertis, R. Pandya, L. A. Muscarella, N. Sawhney, N. Malgorzata, B. Ehrler, A. Rao *et al.*, The impact of exciton delocalization on exciton-vibration interactions in organic semiconductors (2020), https://doi.org/10.17863/CAM.56205.

[57] http://www.hpc.cam.ac.uk.